HUMAN GENE THERAPY 26:14–25 (January 2015)

DOI: 10.1089/hum.2014.015

Intratumoral Injection of Ad-ISF35 (Chimeric CD154) Breaks Tolerance and Induces Lymphoma Tumor Regression

Mauricio Urquiza,[1,2,*] Johanna Melo-Cardenas,[1,2,*] Robier Aguillon,[1,2] Thomas J. Kipps,[1,2,†] and Januario E. Castro[1,2,†]

Abstract

Ad-ISF35, an adenovirus vector encoding a membrane-bound engineered CD154 chimeric protein (ISF35), induces complete A20 lymphoma tumor regression in mice after intratumoral direct injection (IDI). Ad-ISF35 induced durable local and systemic antitumor responses associated with a rapid tumor infiltration of macrophages and neutrophils as well as increased levels of proinflammatory cytokines in the tumor microenvironment. Ad-ISF35 IDI transduced preferentially fibroblasts and macrophages present in the tumor microenvironment, and ISF35 protein expression was observed in only 0.25% of cells present in the tumor. Moreover, Ad-ISF35 IDI induced upregulation of CD40 in tumor and immune regulatory cells, including those that did not express ISF35, suggesting the presence of a strong bystander effect. These responses resulted in the generation of IFN-γ-secreting cytotoxic lymphocytes and the production of specific cytotoxic antibodies against lymphoma cells. Overall, cellular immune therapy based on ISF35 induced phenotypic changes in the tumor cells and tumor microenvironment that were associated with a break in tumor immune tolerance and a curative antitumor effect in this lymphoma mouse model. Our data highlight the potential activity that modulation of costimulatory signaling has in cancer therapy.

Introduction

The tumor microenvironment protects cancer cells from an immune attack by generating immunosuppressive signals that target effector and dendritic cells. These signals are mediated by cell–cell contact or the release of immunomodulatory molecules and cytokines.[1,2] CD40 can help to restore the immune responses against the tumor through interaction with its ligand, CD154. CD40 is a member of the tumor necrosis factor receptor superfamily and is broadly expressed by immune, hematopoietic, vascular, epithelial, and a wide range of cancers, such as breast, lung, prostate, and lymphomas, among others.[3] CD154 is expressed upon activation by T cells, monocytes, and endo thelial cells.[4–6] CD40-CD154 interaction normally plays an important role by inducing the activation of innate and adaptive immune responses.[5] On the other hand, activation of CD40 mediated by CD154 has been shown to induce cell death in different preclinical studies.[7]

Tumor cells stimulated with CD154 restore or even increase the expression of immunomodulatory molecules and also become more sensitive to T-cell-mediated cytotoxicity.[8] Moreover, CD154 is able to induce tumor regression and protection against subsequent tumor re-implantation.[4,9,10] Indeed, the CD40-CD154 signaling pathway has been used with encouraging results as a target for cancer therapy in different models, including leukemia, lymphomas, and gastric and bladder cancer, among others.[3,11–17]

We have previously reported the use of an adenovirus vector that encodes mouse CD154 (Ad-mCD154) in patients with chronic lymphocytic leukemia (CLL).[18] Transduction of CLL cells with Ad-mCD154 enhances their ability to function as antigen presenting cells by inducing the upregulation of important costimulatory molecules such as CD80, CD86, CD54, CD40, and MHC class I and II. These costimulatory molecules activate T cells promoting their cytotoxic activity. However, the biological activity of Ad-mCD154

[1]Moores Cancer Center, University of California–San Diego, La Jolla, CA 92093-0820.
[2]CLL Research Consortium, University of California–San Diego, La Jolla, CA 92093-0820.
*These two authors contributed equally to this work.
†These two senior authors contributed equally to this work.

decreases over time because of a rapid metalloprotease (MMPs) cleavage of this molecule from the transduced cell membrane and the induction of anti-mCD154 blocking antibodies.[18] The use of human CD154 could circumvent the blocking antibody problem. However, expression of human CD154 in neoplastic and normal cells is challenging because of the presence of particular sequences in the carboxy-terminal domain and other unknown factors that cause a very transient membrane expression.[19]

To overcome these difficulties we engineered ISF35, a chimeric human-mouse CD154 homolog molecule with amino acid substitutions within the carboxy-terminal and deletion of the metalloprotease cleavage site, to achieve persistent membrane-bound ISF35 expression. In our initial Ad-ISF35 clinical trials, CLL patients treated with infusions of Ad-ISF35-transduced autologous leukemia cells tolerated well this intervention. They also showed objective clinical benefits, including decrease in leukemia cell counts from the peripheral blood and regression of lymphadenopathy and splenomegaly.[20] Moreover, we have demonstrated that CLL patients benefit clinically not only from administration of autologous Ad-ISF35-transduced leukemia cells, but also from immune modulation mediated by Ad-ISF35 intranodal direct injection.[17] Patients who received these injections tolerated well the procedure with no serious adverse events and with significant clinical improvement.[17]

The antitumoral activity of Ad-ISF35 intratumoral direct injection (IDI) was recapitulated in the immunocompetent mouse model, where we observed that mice bearing large A20 lymphoma tumors were completely cured after intratumoral injection of Ad-ISF35.[21] The Ad-ISF35 activity depends on vector accumulation primarily in the injected tumors with a biodistribution pattern that showed rapid clearance and no evidence of Ad-ISF35 accumulation or persistence in the injected tumor or peripheral organs.[21] Preliminary evidence from this and other unpublished works suggests that the ISF35 immunomodulation involves not only the tumor cells but also cells from the microenvironment. However, the cellular and molecular mechanisms involved in this process are unknown. In order to dissect the molecular mechanism involved in the activation of the immune system that results in the A20 tumor eradication, we conducted additional experiments using Ad-ISF35 IDI in A20 lymphoma BALB/c mice.

Materials and Methods

Cell lines

A20 lymphoma cells were obtained from the American Type Culture Collection (ATCC, Rockville, MD) and were cultured in RPMI 1640 supplemented with 10% FBS.

A20 lymphoma tumor mouse model

Animal procedures were performed in accordance with the guidelines of the Institutional Animal Care and Use Committee. The injection site of recipient animals (BALB/c) was shaved and wiped with 70% ethanol. A20 cells were washed twice in phosphate-buffered saline (PBS), counted, and checked for viability by trypan blue exclusion. A suspension of 1×10^5 viable cells in 100 μl of PBS per mouse was prepared for subcutaneous tumor implantation. After 14 days, more than 90% of mice displayed palpable tumor covering a volume of 65 mm^3. Mice were randomly divided into three groups receiving IDI of the vehicle (PBS), Ad-ISF35 (3×10^{10} vp), or Ad5 (3×10^{10} vp). Tumor growth was measured twice a week. Tumor length and width were measured using a caliper. Tumor volumes were calculated by (length$\times$ width^2)/2. In the case that another tumor was observed in a mouse, it was also measured and its volume was added.

Identification and isolation of tumor cell populations

Mice bearing A20 tumors ($n=3$) on right and left flank were injected with Ad-ISF35 (3×10^{10} vp in 100 μl of PBS). Four hours after injection, mice were sacrificed and tumors were dissociated using Liberase (Roche, Indianapolis, IN) 0.5 mg/ml in HBSS (Invitrogen, Carlsbad, CA) for 30 min at 37°C. Then, tissue debris was filtered using cell strainers (100 μm) and cells in suspension were washed 3 times with RPMI + 10% FBS. Cells were then incubated with anti-mouse CD16/32 (BD Biosciences, San Jose, CA) for 20 min at 4°C. Depletion of B220-positive cells was performed using anti-B220 biotinylated antibody (BD Biosciences) 1/2000 dilution for 15 min at 4°C followed by incubation with Dynabeads MyOne streptavidin beads (Invitrogen). Cells were magnetically removed, and supernatant was collected and washed. Antibodies antimouse GR-1, F4/80, B220, CD45, CD121a, CD31, CD3, CD49b, CD11c, and propidium iodide (BD Biosciences) were used to stain tumor cells for 30 min at 4°C. Cells were sorted in a FACS Aria II, and data analysis was performed using FACS Diva. Dead cells (propidium iodide positive) were excluded and the following cells were sorted in 500 μl of FBS: macrophages ($GR1^-$ $F4/80^+$ $B220^-$), immature myeloid cells ($GR1^{Dim}$ $F4/80^+$ $B220^-$), granulocytes ($GR1^+$ $F4/80^-$ $B220^-$), B cells ($GR1^-$ $F4/80^-$ $B220^+$), fibroblasts ($CD45^-$, $CD121a^+$, $CD31^-$), NK cells ($CD3^-$, $CD49b^+$, $CD11c^-$), NK-T cells ($CD3^+$, $CD49b^+$, $CD11c^-$), myeloid cells ($CD3^-$, $CD49b^-$, $CD11c^+$), and T cells ($CD3^+$, $CD49b^-$, $CD11c^-$). Cells were then washed twice with PBS, and pellet was dried and frozen at -80°C until use.

Quantification of Ad-ISF35 in isolated cells

Cell pellets were resuspended in molecular-grade water and used for Ad-ISF35 amplification using qPCR standardized to detect at least 5 Ad-ISF35 copies in 100 ng of DNA ($\sim$17,000 cells) following FDA guidelines.[22] All samples were tested in duplicate with less than 5% variability. Bone marrow cells from a vehicle-injected mouse were used as a negative control. The following primers specific for detecting only Ad-ISF35 (not CD154 from mouse or human origin) were used:

Forward, 5′CCT CTG GCT GAA GCC CAG3′ (400 n*M*)

Reverse, 5′CTC CCA AGT GAA TGG ATT GT3′ (400 n*M*)

TaqMan MGB-FAM probe, 5′TTACTCAAGGCGG CAAA3′ (250 n*M*).

TaqMan qPCR Universal Master Mix w/UNG from Applied Biosystems (Foster City, CA) was used for the PCR amplification in a BioRad cycler iQ5 PCR machine. The program employed a denaturation step at 95°C for 3 min and 40 cycles of amplification steps at 95°C for 20 sec and 52°C for 1 min and 20 sec. Ad-ISF35 copy number was calculated using Applied Biosystems protocol.[23] A false-positive signal

was excluded when the Ct value was greater than the Ct value for our level of sensitivity (5 AdISF35 copies).

Evaluation of cell surface markers by flow cytometry

Tumor cells were dissociated by using cell strainers and counted, and cell density was adjusted to 10 million cells/ml with PBS supplemented with 1% BSA and 0.05% sodium azide (FACS buffer). For cell surface staining, cells were incubated for 30 min (4°C) with antibodies to CD54, CD80, CD86, CD3, CD4, CD8, CD25, GR1, CD11b, CD11c, CD14, CD154, and CD95 (BD Biosciences). Cells were then washed and resuspended in FACS buffer, and their fluorescence data were acquired using a FACSCalibur flow cytometer (Becton Dickinson, San Jose, CA). Analysis gates were placed on the target populations, and percentages of cells were evaluated using Flow-Jo software (TreeStar, Ashland, OR).

Cytokine levels in tumor and serum samples

Sera were collected from terminal blood draws of A20 tumor-bearing mice and frozen at −20°C until use. Tumor and spleen samples were disrupted using cell strainers in presence of 100 μl of HBSS (Invitrogen). Samples were then centrifuged and tumor milieu was stored at −20°C. Cytokine levels of IL-2, IL-6, IL-10, IL-12 (p70), MCP-1, GM-CSF, and IFN-γ were measured using Luminex xMAP technology. Briefly, 25 μl of either serum or tumor/spleen milieu was incubated with premixed microspheres for 1 hr at room temperature followed by two washes with wash buffer by vacuum filtration. Then, 25 μl of detection antibodies was added and incubated for 30 min at room temperature, and 25 μl of streptavidin–phycoerythrin was added to each well and incubated for 30 min at room temperature. Nonspecific binding was removed by washing two times. Beads were then resuspended in 200 μl of sheath fluid and fluorescence intensity was measured in Luminex 100 IS machine. Cytokine levels were analyzed by spline curve-fitting method using BeadView software version 1.0.

Immunohistochemistry analysis

Tumor samples were obtained 24 hr after mice were injected with the vehicle, Ad5, or Ad-ISF35. As a control, a group of mice was injected with Ad-ISF35 heat inactivated at 70°C for 1 hr. Tumors were collected and frozen in OTC compound (VWR, San Dimas, CA). Sections were stained with antibodies anti-CD3, F4/80, CD31, GR1, and Mac1. Microscopic evaluation was performed using a Nikon Eclipse E800 microscope and objectives as listed in the figure legends (Nikon, Melville, NY). Images were captured with a SPOT RT color model 2.2.1 camera and analyzed using SPOT software version 3.5 (Diagnostic Instruments, Sterling Heights, MI).

Antibody-dependent cytotoxicity assay

Mice bearing A20 lymphoma tumors were treated with the vehicle, Ad5, or Ad-ISF35 and sacrificed 2 weeks after third injection with the vehicle, Ad5, or Ad-ISF35. Serum samples and splenocytes were collected. A20 cells growing in culture were washed twice with PBS and stained with PKH67 (Sigma, St. Louis, MO) following manufacturer's instructions. Labeled A20 cells were cultured with inactivated serum samples and splenocytes at different ratios in AIM-V media (Invitrogen). Cell death was measured by PI staining in a FACSCalibur flow cytometer (Becton Dickinson) and data were analyzed using Flow Jo (TreeStar).

Complement-dependent cytotoxicity assay

A20 cells were cultured for 1 hr at 37°C with 10% serum obtained from mice described above in the antibody- dependent cytotoxicity (ADCC) assay. As a negative control, serum was inactivated at 60°C for 1 hr. Cell death was measured by PI staining.

Western blot

A20 cells were lysed with RIPA buffer (Sigma) supplemented with protease and phosphate inhibitors for 30 min at 4°C. Lysates were then centrifuged, and supernatant was collected and quantified using Bradford assay (BioRad, Hercules, CA). An amount of 100 ng of protein was loaded in 4–12% polyacrylamide gel having a single well and transferred to nitrocellulose membranes. For blocking unspecific interactions, BSA 1% in TBS was used for 1 hr at room temperature. Using the MPX Multiplexer blotting system (LI-COR, Lincoln, NE), serum samples obtained from mice described in the ADCC section were diluted 1/200 in TBS–BSA 1%–Tween 0.05% and incubated over night at 4°C. After five washes with TBS–Tween 0.05%, membranes were incubated with 1/5000 dilution of HRP-conjugated antimouse IgG antibody (Pierce, Rockford, IL). Subsequent development was performed using Super Signal West Femto Chemiluminescent Substrate (Pierce) and autoradiography was performed with Kodak scientific imagining films.

ELISPOT assay

Ninety-six-well PDVF membrane plates were coated with antimouse IFN-γ antibody 1/500 (BD Biosciences) over night at 4°C. After three washes with PBS–Tween 0.05% (PBS-T), splenocytes collected as described in ADCC section were cultured at different ratios with A20 cells in AIM-V media (Invitrogen) for 48 hr. Then, cells were removed and membrane was washed three times with PBS-T. Developing antibody labeled with alkaline phosphatase was then added at 1/500 dilution and incubated for 2 hr at room temperature. After washing, plates were incubated with TMB substrate for 30 min. Plates were then washed with water and dried for subsequent count. CTL-Immunospot reader (Cellular Technology Limited-CTL, Shaker Heights, OH) was used for automated counting.

Statistical analysis

Data were analyzed using a two-tailed Welch's Student *t*-test or one-way ANOVA test except for survival curves, which were analyzed using the log-rank test. All analyses were performed using Prism software (GraphPad, San Diego, CA).

Results

Intratumoral administration of Ad-ISF35 induced tumor regression and cure of A20 lymphoma BALB/c mice

Ad-ISF35 IDI induced complete tumor regression curing 80% of A20 tumor bearing mice (Fig. 1A). The regression

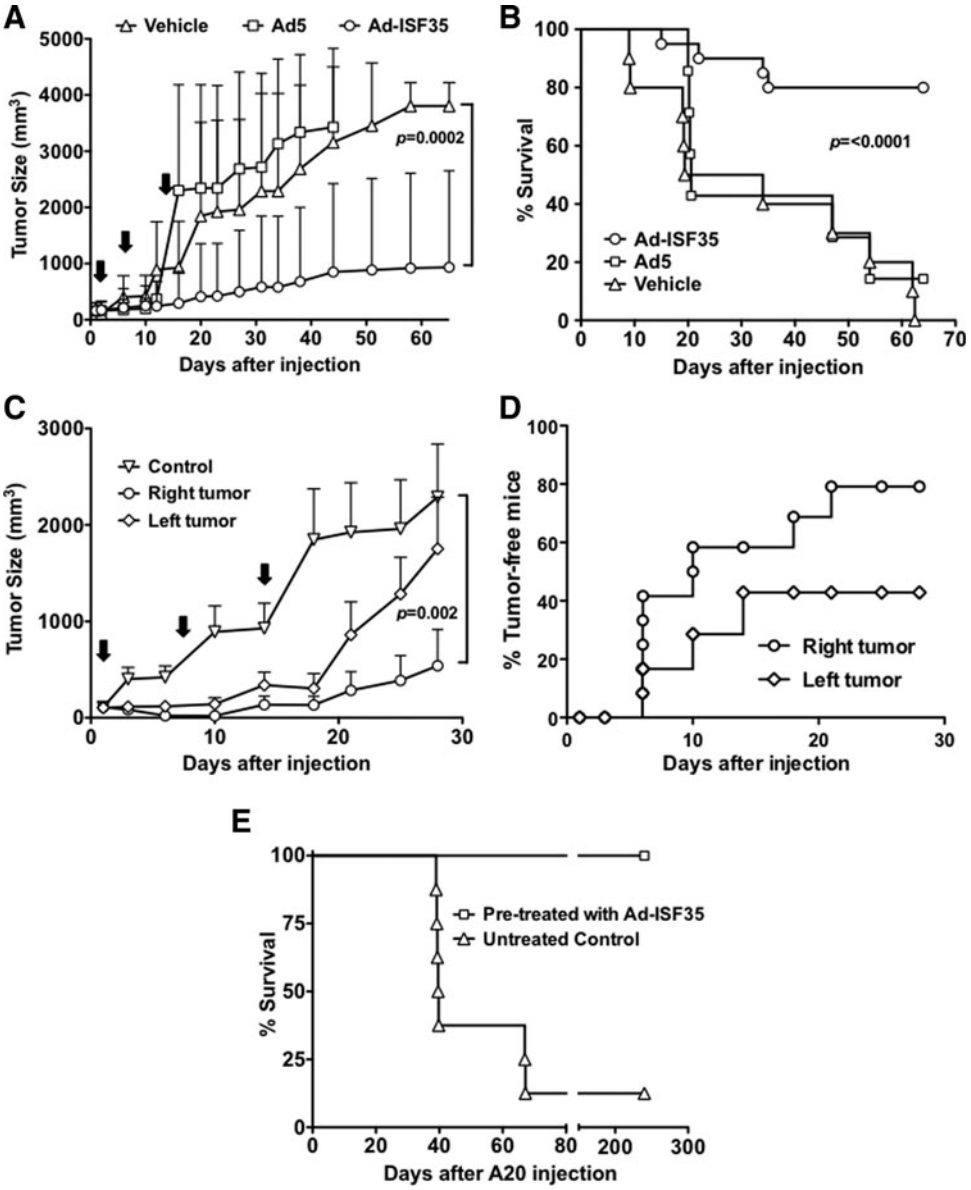

FIG. 1. Ad-ISF35 intratumoral direct injection (IDI) results in tumor regression by inducing local and systemic immune responses. **(A)** A20 tumor-bearing mice received three weekly IDI of the vehicle, Ad5 (3×10^{10} vp), or Ad-ISF35 (3×10^{10} vp) as shown by the arrows. Tumor size was measured over time and statistical analysis was performed. **(B)** Survival curve of mice receiving the vehicle, Ad5, and Ad-ISF35. **(C)** Tumor growth of bilateral injection of A20 cells. The tumor present on the right flank was injected with Ad-ISF35 or the vehicle (control). The tumor on the left was not injected. **(D)** Percentage of tumor-free mice on the right flank (Ad-ISF35 injected) and left flank (noninjected). **(E)** Survival curve of mice rechallenged with A20 cells 3 months after Ad-ISF35 IDI-induced tumor regression. Age-matched control group previously untreated was also injected with the same batch of A20 cells. Error bars indicate the standard deviation.

of A20 subcutaneous tumors was rapid and initiated 2–5 days after the first Ad-ISF35 injection. In contrast, control adenovirus 5 (Ad5) or vehicle-injected tumors continued growing and reached tumor volumes that required sacrifice according to institutional policies (Fig. 1A). After 64 days of follow-up, none of the vehicle- or Ad5 control IDI-treated mice survived, while 80% of Ad-ISF35 IDI-treated mice were still alive with no detectable tumor (Fig. 1B).

We were interested in determining whether or not the antitumoral response elicited by Ad-ISF35 IDI was only local or systemic. Therefore, we implanted subcutaneous bilateral A20 tumors on the right- and left-side flanks. After 14 days, mice were injected with Ad-ISF35 only in the right-side tumors (average tumor size $\sim 62\,mm^3$). Control mice were injected with the vehicle only. Similarly to what we observed in previous experiments, 80% of Ad-ISF35-injected tumors (right side) showed a complete regression in less than 2 weeks. Interestingly, 40% of left-side tumors (noninjected with Ad-ISF35) showed a decreased growth rate and complete regression. All mice injected with the vehicle showed rapid tumor progression and were sacrificed within 2 weeks after injection (Fig. 1C and D).

In order to evaluate whether Ad-ISF35 induced a protective immune response able to reject tumor re-implantation, we challenged with A20 tumor cells mice that were cured after Ad-ISF35 IDI ($n=10$). None of them developed tumors during a follow-up period of 9 months. As a control, matching-age mice ($n=8$) previously untreated were also injected with the A20 cells and tumor growth was measured. All control mice (except one) grew tumors and died between 40–60 days after injection with A20 cells (Fig. 1E).

Ad-ISF35 IDI induces tumor necrosis, edema with architectural distortion, and early infiltration of macrophages and neutrophils

To determine the early changes in tumor structure and the infiltration of immune cells associated specifically to

Ad-ISF35 presence, tumors were analyzed 24 hr after being injected with the vehicle, Ad5, AdISF35, or heat-inactivated Ad-ISF35 by immunohistochemistry. These lymphoma tumors comprised more than 95% of B220-positive cells (Supplementary Fig. S1; Supplementary Data are available online at www.liebertpub.com/hum). We used heat-inactivated virus because it is unable to transduce cells and would allow us to discriminate the effect of ISF35 expression versus nonspecific immune activation mediated by the viral particles. Ad-ISF35-injected tumors showed necrosis causing edema and cell death with distortion of the tumor architecture in ~90% of the tissue analyzed. Interestingly, these histological changes were associated with an intense accumulation of GR-1, and F4/80-positive cells, most likely representing macrophages and neutrophils. Mice injected with Ad5 or heat-inactivated Ad-ISF35 showed a slight increase in F4/80-positive cells probably mediated by viral antigens. However, neither these controls nor the vehicle-injected mice showed the strong histological changes or amount of cellular infiltrates as observed with Ad-ISF35 (Fig. 2). Staining for T cells ($CD3^+$) and $CD11b^+$ (myeloid cells) were also performed and did not show major changes in the tissues injected with Ad-ISF35 or controls at this early time point (24 hr). However, as shown later, the infiltration of T cells in Ad-ISF35-treated tumors was a late event that was observed after 48 hr (Fig. 5A).

Immunohistochemistry analysis after 24 hr was not possible because of massive necrosis and tumor destruction observed after Ad-ISF35 IDI. Therefore, we used flow cytometry to analyze tumor cells beyond 24 hr post-IDI.

A more detailed analysis of these tumors by flow cytometry showed an increase in the percentage of macrophages and myeloid cells. Myeloid cells ($CD11b^+GR1^+$) were increased in tumors injected with Ad5 and Ad-ISF35, but it was only statistically significant in the Ad-ISF35 IDI group (Fig. 3A). These myeloid cells expressed low and high levels of GR1 but we did not observe changes in the proportion of these populations (data not shown).

Expression of chimeric CD154-ISF35 induces cellular activation in the tumor microenvironment

In order to determine which cell types are transduced by Ad-ISF35, we analyzed the copy number of Ad-ISF35 vector in different subsets of A20 tumor cells sorted by flow cytometry 4 hr post-IDI. High *Ad-ISF35* DNA copy number was detected almost exclusively in fibroblasts (~400 vector copies/10,000 sorted cells) and macrophages (~300 vector copies/10,000 sorted cells) (Fig. 3B). Myeloid cells were also positive for *Ad-ISF35* DNA; however, the frequency was much lower. A very low copy number of *Ad-ISF35* DNA was detected in A20 tumor cells ($B220^+$), NK-T cells, T cells, and granulocytes (< 10 vector copies/10,000 sorted cells).

In addition, we performed flow cytometry analysis to determine the level of expression of ISF35 (chimeric CD154 molecule) in the injected tumors. Tissue samples from tumors injected with Ad-ISF35 and controls were analyzed at 12 and 48 hr postinjection. Expression of ISF35 was low (0.1%) and was not statistically different among the different tumor samples analyzed at 12 hr postinjection. However, at 48 hr there was a statistically significant increase in the level of expression (~0.25%) in tumor samples from mice treated with Ad-ISF35 IDI (Fig. 3C).

Subset analysis of ISF35 expression in different tumor cells revealed that macrophages were the cell type that

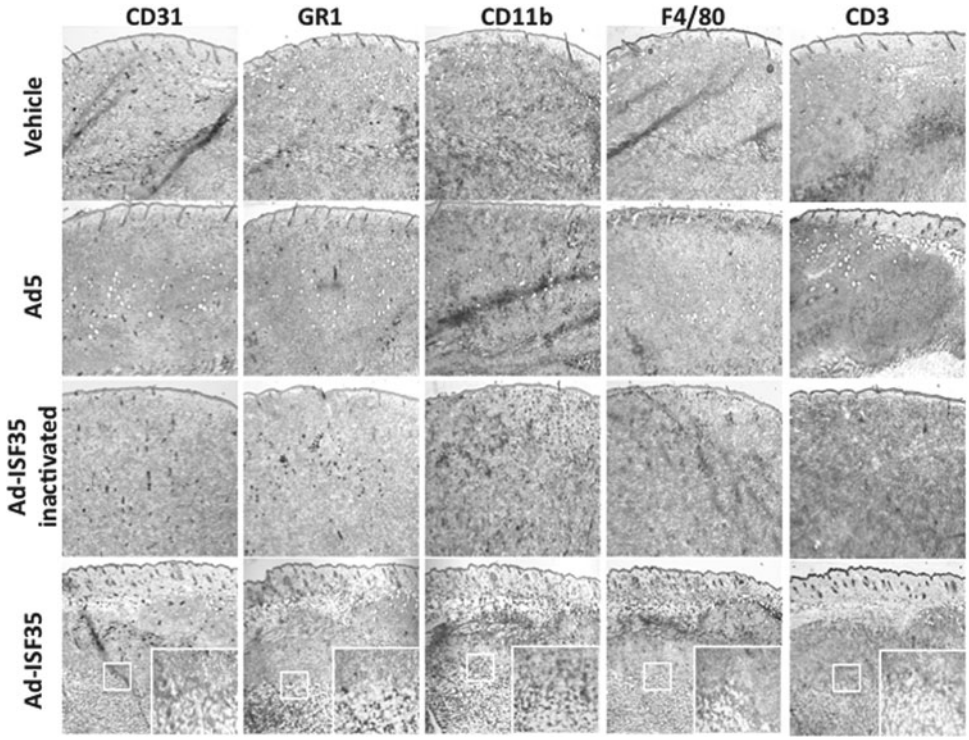

FIG. 2. Ad-ISF35 induces A20 tumor necrosis and early infiltration of neutrophils and macrophages. Immunochemistry analysis of tumors harvested 24 hr after IDI with Ad-ISF35, Ad5, vehicle, and Ad-ISF35 heat inactivated at 72°C for 1 hr. Staining with anti-CD31 (endothelial cells), anti-GR1 (macrophages and neutrophils), anti-CD11b (granulocytes, macrophages, and monocytes), anti-F4/80 (macrophages), and anti-CD3 (T cells) antibodies is shown. Color images available online at www.liebertpub.com/hum

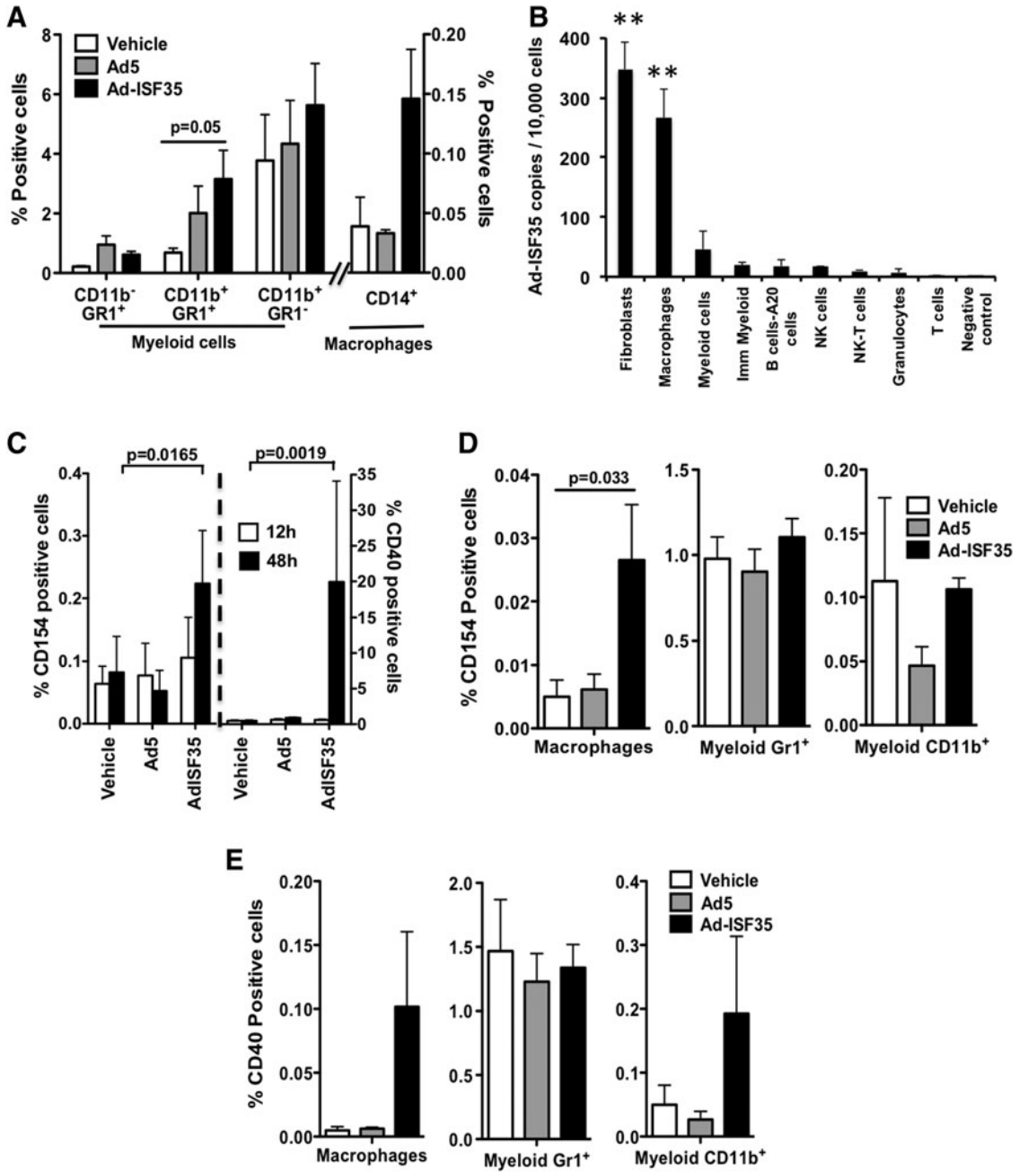

FIG. 3. Expression of chimeric CD154- ISF35 induces cellular activation in the tumor microenvironment. **(A)** Flow cytometry analysis of the percentage of myeloid cells and macrophages present in the tumor 48 hr after Ad-ISF35 IDI. **(B)** Ad-ISF35 DNA copy numbers per 10,000 cells was measured by qPCR in different tumor cell types 4 hr after Ad-ISF35 IDI. Asterisks indicate a $p < 0.01$ compared with the other cell types. Bone marrow cells from mice treated with the vehicle were used as a negative control. **(C)** Tumors injected with the vehicle, Ad5, or Ad-ISF35 were harvested 12 and 48 hr after IDI. Cells were dissociated and flow cytometry was performed. Analysis of CD40 and CD154 was performed in all the tumor population. A more detailed analysis was performed on macrophages and myeloid cells expressing CD154 **(D)** and CD40 **(E)**. Error bars indicate the standard deviation. Statistical analysis was performed using *t*-test with Welch's correction.

expressed ISF35 the most after *Ad-ISF35* IDI (Fig. 3D), in accordance with the high level of Ad-ISF35 DNA copy number expression observed in these cells (Fig. 3B). Other myeloid cells (GR1 or CD11b positive) had lower levels of ISF35 expression that did not change significantly compared with control injections (Fig. 3D).

Based on the *Ad-ISF35* vector copy number distribution, we expected to see a high level of ISF35 expression in fibroblasts (Fig. 3B). However, the absolute number of fibroblast present in the tumors analyzed was too small (<0.08%) that we were unable to reliably quantify surface expression markers on these cells.

Because the of the low frequency of tumor cells infected with Ad-ISF35 and the rapid clearance of the virus in less than 48 hr,[21] it is very likely that the activity of Ad-ISF35 requires amplification of cellular activation mediated by expression of proteins, including costimulatory molecules. To evaluate this cellular activation effect, we assessed the expression of CD40 in tumors after IDI. Cells from Ad-ISF35-injected tumors showed the highest levels of CD40 expression that were statistically significant at 48 hr compared with Ad5- and vehicle-injected controls (average expression of 20% in Ad-ISF35-injected tumors vs. $<1\%$ Ad5/vehicle controls) (Fig. 3C). We observed that $CD14^+$ cells (mainly macrophages) and myeloid $CD11b^+$ cells from Ad-ISF35-injected tumors showed an increase of CD40 expression compared with control injections; however, this was not statistically significant (Fig. 3E). CD40-expressing cells most likely correspond to A20 lymphoma cells.

Ad-ISF35 IDI induced release of chemokines and proinflammatory cytokines into the tumor microenvironment

Ad-ISF35 induced the recruitment and activation of cells from the tumor microenvironment (Figs. 2 and 3). This could be mediated by cell-to-cell interactions or by means of release of soluble factors. To evaluate this, we measured levels of different cytokines and chemokines in the tumor, spleen, and serum of mice that received Ad-ISF35 IDI or controls. We found that IL-6, IL-12, and GM-CSF were increased in the tumors from mice that received Ad5 and Ad-ISF35 IDI compared with vehicle control. The expression was detected as early as 12 hr postinjection but appeared to last longer in Ad-ISF35-injected tumors since they were still detectable at 48 hr. In the spleen we found increased IL-6 and MCP-1 levels in mice receiving either Ad-ISF35 or Ad5. There was a significant early increase in serum IL-2, IL-6 in mice treated with Ad5 or Ad-ISF35 but not the vehicle. Only Ad5-treated mice showed increased levels of IL-10 in serum (Fig. 4).

Ad-ISF35 induces a time-dependent tumor infiltration of T lymphocytes

Because the repertoire of T cells is strongly associated with immunoactivation or immunosuppression, we analyzed the profile of T cells that infiltrated the tumors after IDI. Interestingly, there was a significant increase in $CD3^+$ T cells (both $CD4^+$ and $CD8^+$) after Ad-ISF35 IDI that was observed after 48 hr postinjection. T-cell tumor infiltration was not observed after Ad5 control IDI (Fig. 5A). In addition, $CD3^+CD8^+$ lymphocytes from Ad-ISF35-injected tumors showed an activation phenotype ($CD25^+$) that was significantly increased compared with those T cells found in control tumors (Fig. 5B).

Ad-ISF35 IDI elicited a break in tumor tolerance with development of cellular and humoral immune responses against A20 cells

We evaluated the role of cellular and humoral immune responses elicited by IDI in this lymphoma model. Our experiments showed that Ad-ISF35 IDI but not controls induced antibody production against A20-derived antigens (Fig. 5C). Moreover, serum from Ad-ISF35-treated mice induced apoptosis in approximately 50% of A20 cells, while this was not observed when lymphoma cells were incubated with sera from mice injected with control Ad5, vehicle, or heat-inactivated serum from Ad-ISF35-treated mice. This suggests that Ad-ISF35 IDI induced tumor-specific antibodies capable of eliciting complement-dependent cytotoxicity of A20 cells (Fig. 5D).

Spleen cells obtained from mice treated with the vehicle, Ad5, or Ad-ISF35 were tested *in vitro* for their ability to induce a cytotoxic effect against A20 cells by measuring apoptosis and IFNγ production. The results showed that spleen cells from Ad-ISF35-treated mice, but no controls, induced statistically significant higher levels of apoptosis in A20 cells with a cytotoxic activity that was effector-to-target ratio dependent (Fig. 5E). Similarly, only spleen cells obtained from Ad-ISF35-treated mice produced IFNγ *in vitro* as detected by ELISPOT assay in mixed lymphocyte reactions (Fig. 5F).

Discussion

Our results show that ISF35 (a recombinant chimeric CD154 molecule) delivered intratumorally using a replication- deficient adenovirus 5 induced a strong immune activation resulting in complete A20 tumor regression in 80% of mice. This process was associated with both a break in tumor tolerance and the development of durable cellular and humoral immune responses against A20 lymphoma cells. These durable immune responses also protected mice from tumor reimplantation. Ad-ISF35 induced A20 tumor cell death, which was detectable 2 days after injection. This effect appears to be systemic as it was present not only in tumors directly injected with Ad-ISF35 but also in a significant number (40%) of contralateral/simultaneously implanted tumors.

The intratumoral effect of Ad-ISF35 was determined in mice carrying A20 lymphoma that expresses CD40 but does not express CD154.[24] Activation of CD40 by Ad-CD154 on A20 cells results in tumor growth inhibition and induction of apoptosis.[10,21] The robust phenotypic changes induced by CD154 expression include upregulation of Fas (CD95) and costimulatory molecules such as CD80, CD86, and CD54, which are associated not only with apoptosis but also with enhanced antigen presentation capabilities.[19] These phenotypic changes are likely responsible for the antilymphoma effect observed in the Ad-ISF35-treated mice. However, our data suggest that Ad-ISF35 induced expression of chimeric CD154-ISF35 mainly in macrophages and fibroblasts present in tumor microenvironment rather than in A20 lymphoma cells that represented $>90\%$ of the tumor cells.

It is possible that other tumor stromal cells, such as endothelial cells, could also be transduced by Ad-ISF35, as it is well known that adenovirus can infect those cells relatively easy at a low multiplicity of infection.[25] Activation of these cells or the solely expression of ISF35 on their membrane surface may have led the infiltration of neutrophils and monocytes/macrophages during the first 24 hr after Ad-ISF35 injection. These tumor-infiltrating neutrophils and macrophages play an important role in destruction, necroptosis, and removal of tumor cells, a process that is typically impaired in the tumor microenvironment.[26,27] Upon activation, neutrophils and macrophages release the

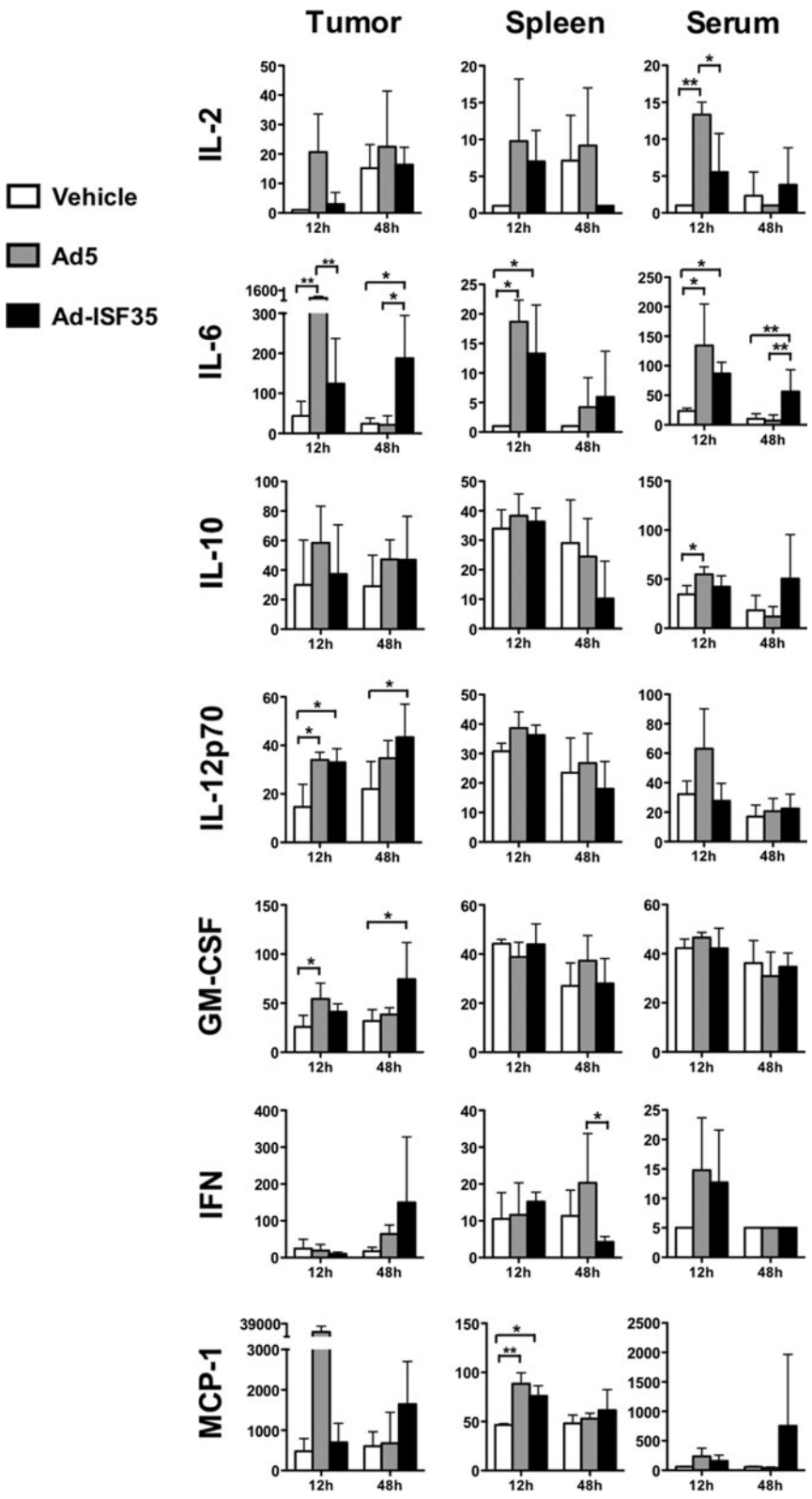

FIG. 4. Ad-ISF35 IDI induces cytokine and chemokine release from the tumor microenvironment and spleen. We evaluated the level of expression of IL-2, IL-6, IL-10, IL12, GMCSF, IFNγ, and MCP-1 (pg/ml), among others, in samples collected from tumor, spleen, and serum from A20-bearing mice that received the vehicle, Ad5, or Ad-ISF35 IDI. The level of expression was quantified using the Luminex platform as described in the Materials and Methods section. Statistical analysis was performed using *t*-test with Welch's correction. $*p < 0.05$; $**p < 0.01$.

content of its granules that are cytotoxic for tumor cells, resulting in the exposure of tumor-associated antigens that can be presented through MHC-I and -II initiating an adaptive immune response.[16,26] Additionally, monocytes/macrophages could have been recruited to the tumor site by the recognition of adenovirus particles, and then activated through ISF35/CD40 interaction with tumor stromal cells. Indeed, CD154 expression mediates the activation of dendritic cells, macrophages, fibroblasts, and/or endothelial cells.[28] CD154/CD40 interaction activates macrophage antitumor

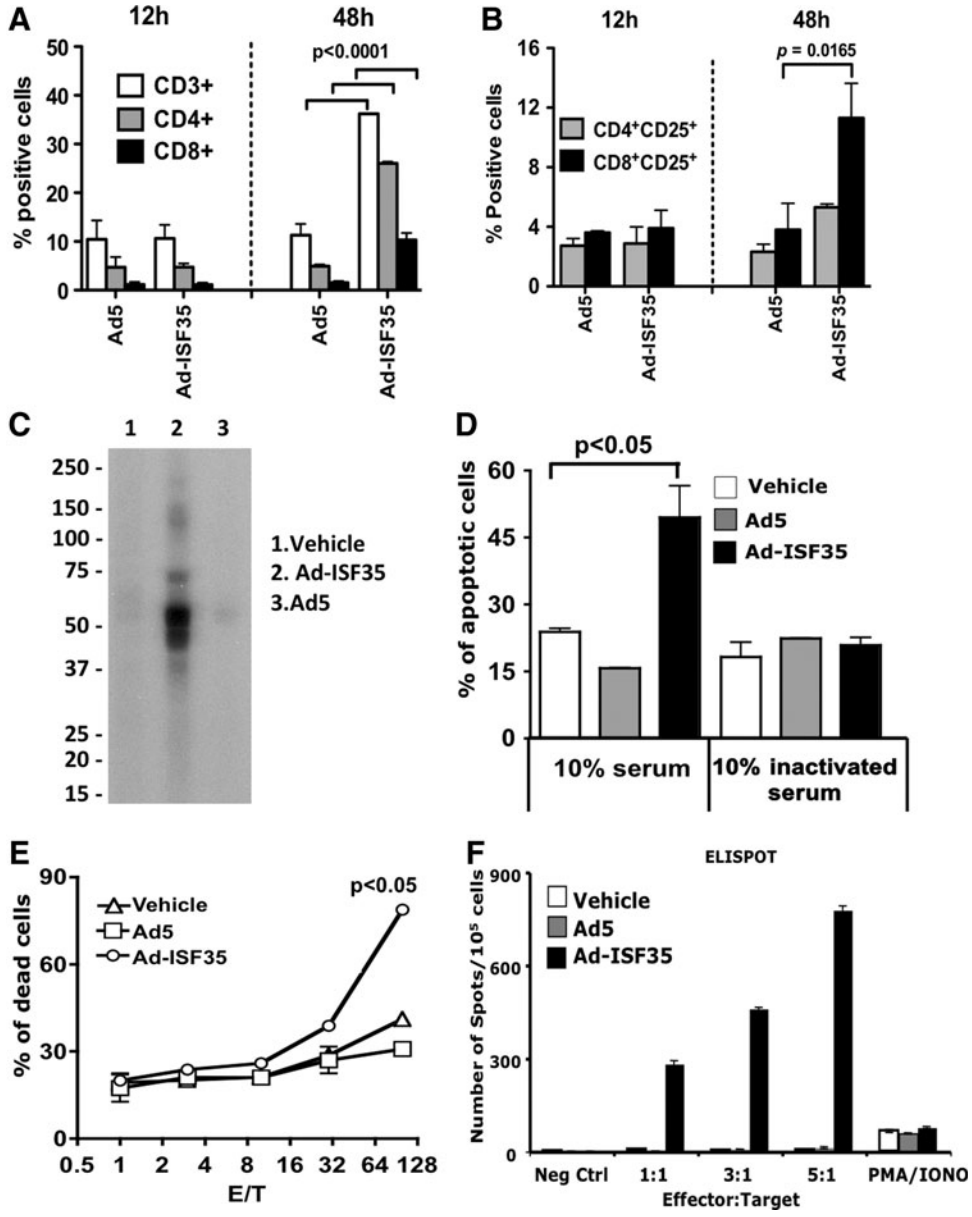

FIG. 5. Ad-ISF35 IDI-mediated induction of late T-cell infiltration and humoral–cellular immune response. **(A)** Analysis of tumor-infiltrating lymphocytes and **(B)** their expression of CD25. **(C–F)** Serum and splenocytes from mice cured by Ad-ISF35 treatment were tested *in vitro*. **(C)** Sera from Ad-ISF35-treated mice, but not control animals, contained antibodies that recognize A20-derived tumor proteins detected by Western blot. A single-well electrophoresis was performed with A20 protein lysate. **(D)** Complement-dependent cytotoxicity (CDC) of A20 cells was determined using sera from A20-bearing mice treated with the vehicle, Ad5, or Ad-ISF35. As a control, serum was inactivated at 56°C for 1 hr. **(E)** A20 cell apoptosis induced by splenocytes from vehicle-, Ad5-, or Ad-ISF35-treated mice at different effector (*E*)-to-target (*T*) ratios was determined by flow cytometry. **(F)** Splenocytes from vehicle-, Ad5-, and Ad-ISF35-treated mice were cultured with A20 cells, and IFN-γ production was determined by ELISPOT. Statistical analysis was performed using *t*-test with Welch's correction.

activity through IFN-γ, TNF receptor, and production of IL-1, IL-6, IL-12, and TNF-α, resembling classically activated effectors/M1 phenotype.[29–31]

It has been previously reported that CD40 ligation is not enough to induce a cytotoxic antitumoral response. Macrophages need an additional ''triggering'' signal, such as CpG and LPS, to become fully activated.[32] In our study, it is very likely that the second signal that triggers the activation of macrophages is the adenoviral particles. However, this triggering signal alone does not seem to induce antitumor responses. Mice treated with Ad5 showed a slight increase in macrophages infiltrating the tumor and production of GMCSF, IL6, and IL12 at early time points. Nevertheless, this effect was not enough to induce tumor regression. In contrast, AdISF35-treated mice showed a dramatic increase in infiltrating macrophages, a long-lasting production of GMCSF, IL6, and IL12 and infiltration of T cells into the tumor, resulting in tumor regression. Therefore, CD40 ligation and the ''triggering'' signal together seem to be necessary to activate macrophages resulting in antitumoral responses. These activated cells will amplify the immune response not only through the expression of these cytokines but also by inducing the expression of molecules that mediate adhesion of neutrophils, monocytes, and lymphocytes to the tumor-activated epithelial cells in the vessel wall.[33,34] Moreover, CD11b/CD18 (Mac-1), an integrin expressed abundantly on monocytes/macrophages, is able to bind CD154 enhancing monocyte adhesion and locomotion.[35] It is possible that the interaction between ISF35 and CD11b increases *in vivo* leukocyte recruitment toward the tumor.

We observed an increase of cells positive for GR1 and CD11b after Ad-ISF35 IDI, which are considered myeloid-derived suppressor cells (MDSCs). MDSCs have been associated not only with tumor progression but also with T-

cell dysfunction and tumor immunotolerance.[36,37] In our model, these cells expressed low and high GR1 levels that have been associated with monocytic and granulocytic myeloid cells, respectively. Recently, Liljenfeldt et al.[38] reported that CD40L treatment induces the shift of myeloid-suppressor cells into a granulocytic subpopulation and this was associated with decreased tumor burden. Therefore, it is likely that AdISF35 is capable of inducing a switch of these cells present in the tumor microenvironment from a suppressive state to an active phenotype. However, we did not observe a shift of these populations in the time points we analyzed in this study.

Interestingly, despite the low percentage of cells expressing ISF35 (0.25%) after Ad-ISF35 injection, we observed tumor regression in 80% of mice. This provides strong evidence of a potent bystander *trans*-activation effect in the tumor microenvironment that contributes to the formation of robust antitumor responses. Our findings are in agreement with other authors who have shown potent immune responses mediated by low levels of CD154 expression.[39] Amplification of *trans*-activation signals mediated by few cells expressing ISF35 in the tumor stroma could be because of a strong bystander effect facilitated by highly mobile macrophages and the expression of proinflammatory cytokines in the tumor microenvironment after Ad-ISF35 IDI.

We observed that GMCSF, IL-6, and IL-12 were expressed at 48 hr after AdISF35 IDI, unlike Ad5-treated mice. This suggests that Ad-ISF35 induces a later/prolonged expression of these cytokines necessary to induce tumor regression. Release of GMCSF could be in part responsible of the increase of CD40 expression.[40] IL-12 plays an important role bridging innate and adaptive immune responses by promoting function of cytotoxic cells and differentiation of T-helper cells.[41] It has been reported that defective IL-12 production impairs antitumor response in the absence of CD40/CD154 interaction. This model is supported by the fact that CD40/CD154 interaction induces activation not only directly by cell–cell contact but also indirectly by releasing soluble mediators.[42]

Increasing numbers of $CD3^+CD4^+$ and $CD3^+CD8^+$ T cells were observed infiltrating tumors injected with Ad-ISF35 but not in controls. Mice injected with Ad-ISF35 that were cured from A20 lymphoma were protected from A20 rechallenge, and their splenocytes induced cytotoxic responses against these lymphoma cells *in vitro*. Interestingly, we observed an increase in the number of cytotoxic T cells and about 10% of them expressed CD25. Expression of CD25 on $CD8^+$ cells has been associated with induction of cytotoxic responses[43] and a memory phenotype.[44] These findings strongly suggest the development of immune memory mediated by both humoral and cellular responses as shown in Figure 5.

The results in this study corroborate our findings in CLL patients who received a single Ad-ISF35 IDI.[17] CLL patients in this trial showed a significant decrease in the size of lymph nodes, spleen, and lymphocytosis with a clinical benefit that was durable and systemic. These changes were associated with an increase in the number of neutrophils in peripheral blood and expression of IFNγ and IL-6. Although we did not obtain lymph node biopsies on these patients, the A20 lymphoma mouse model used here provides a close insight of the cellular and molecular mechanism that could be responsible for the clinical benefit observed in those patients treated with Ad-ISF35 IDI.

In conclusion, intratumoral delivery of Ad-ISF35 induces a complete eradication of lymphoma tumors and long-lasting immunity that involves innate and adaptive responses and break of immune tolerance. We observed that Ad-ISF35 transduced preferentially stromal cells present in the tumor microenvironment rather than A20 tumor cells. These stromal cells induced *trans*-activation of cells present in the tumor microenvironment through a strong bystander effect. In addition, Ad-ISF35 IDI induced cellular activation, including upregulation of CD40 and secretion of cytokines and chemokines such as IL-6, GM-CSF, and IL-12 that promoted tumor infiltration with immune system cells that contribute to tumor regression. Finally, Ad-ISF35 IDI induced antitumoral immune responses that included production of specific antitumoral antibodies and cytotoxic cells. Overall, our findings provide additional evidence of the relevance of the CD154/CD40 pathway as a mediator of potent immune responses and the potential applications of this type of cellular immunotherapy for cancer treatment.

Acknowledgments

We would like to thank Dennis Young from the flow cytometry core at University of California–San Diego (UCSD) for his help with cell sorting and data analysis, and Raymon Araniego and Nissi Varki from the histopathology-shared resources at UCSD for their help with the immunohistochemistry experiments. This work was supported by grants from the Alliance for Cancer Gene Therapy (ACGT) foundation, the Food and Drug Administration (FDA-OOPD-R01-3427 Grant), the Chronic Lymphocytic Leukemia Research Consortium (CRC) NIH (P01 CA081534), UC San Diego Foundation Blood Cancer Research Fund (T.J.K.), and the Bennett Family Foundation (J.E.C.). Memgen LLC provided Ad-ISF35 GMP quality.

Author Disclosure Statement

T.J.K. receives stock options as payment for providing consulting services to Memgen, LLC. The University of California owns the patent for Ad-ISF35 and licenses it to Memgen, LLC. The other authors declare no competing financial interests.

References

1. Draghiciu O, Nijman HW, and Daemen T. From tumor immunosuppression to eradication: targeting homing and activity of immune effector cells to tumors. Clin Dev Immunol 2011;2011:439053.
2. Shiao SL, Ganesan AP, Rugo HS, et al. Immune microenvironments in solid tumors: new targets for therapy. Genes Dev 2011;25:2559–2572.
3. Fonsatti E, Maio M, Altomonte M, et al. Biology and clinical applications of CD40 in cancer treatment. Semin Oncol 2010;37:517–523.
4. Loskog A, Bjorkland A, Brown MP, et al. Potent antitumor effects of CD154 transduced tumor cells in experimental bladder cancer. J Urol 2001;166:1093–1097.
5. Xu Y, and Song G. The role of CD40-CD154 interaction in cell immunoregulation. J Biomed Sci 2004;11:426–438.

6. Ma DY, and Clark EA. The role of CD40 and CD154/CD40L in dendritic cells. Semin Immunol 2009;21:265–272.
7. Rickert RC, Jellusova J, and Miletic AV. Signaling by the tumor necrosis factor receptor superfamily in B-cell biology and disease. Immunol Rev 2011;244:115–133.
8. Blair PJ, Riley JL, Harlan DM, et al. CD40 ligand (CD154) triggers a short-term CD4(+) T cell activation response that results in secretion of immunomodulatory cytokines and apoptosis. J Exp Med 2000;191:651–660.
9. Tong AW, Papayoti MH, Netto G, et al. Growth-inhibitory effects of CD40 ligand (CD154) and its endogenous expression in human breast cancer. Clin Cancer Res 2001;7:691–703.
10. Briones J, Timmerman J, and Levy R. *In vivo* antitumor effect of CD40L-transduced tumor cells as a vaccine for B-cell lymphoma. Cancer Res 2002;62:3195–3199.
11. Wierda WG, Rassenti LZ, Cantwell MD, et al. A phase I study of CD154 (CD40-ligand) gene therapy for chronic lymphocytic leukemia. Blood 1999;94:602a (abstract).
12. Friedlander PL, Delaune CL, Abadie JM, et al. Efficacy of CD40 ligand gene therapy in malignant mesothelioma. Am J Respir Cell Mol Biol 2003;29:321–330.
13. Dessureault S, Noyes D, Lee D, et al. A phase-I trial using a universal GM-CSF-producing and CD40L-expressing bystander cell line (GM.CD40L) in the formulation of autologous tumor cell-based vaccines for cancer patients with stage IV disease. Ann Surg Oncol 2007;14:869–884.
14. Malmstrom PU, Loskog AS, Lindqvist CA, et al. AdCD40L immunogene therapy for bladder carcinoma—the first phase I/IIa trial. Clin Cancer Res 2010;16:3279–3287.
15. Yi Q, Szmania S, Freeman J, et al. Optimizing dendritic cell-based immunotherapy in multiple myeloma: intranodal injections of idiotype-pulsed CD40 ligand-matured vaccines led to induction of type-1 and cytotoxic T-cell immune responses in patients. Br J Haematol 2010;150:554–564.
16. Beatty GL, Chiorean EG, Fishman MP, et al. CD40 agonists alter tumor stroma and show efficacy against pancreatic carcinoma in mice and humans. Science 2011;331:1612–1616.
17. Castro JE, Melo-Cardenas J, Urquiza M, et al. Gene immunotherapy of chronic lymphocytic leukemia: a phase I study of intranodally injected adenovirus expressing a chimeric CD154 molecule. Cancer Res 2012;72:2937–2948.
18. Wierda WG, Cantwell MJ, Woods SJ, et al. CD40-ligand (CD154) gene therapy for chronic lymphocytic leukemia. Blood 2000;96:2917–2924.
19. Cantwell MJ, Wierda WG, Lossos IS, et al. T cell activation following infection of primary follicle center lymphoma B cells with adenovirus encoding CD154. Leukemia 2001;15:1451–1457.
20. Wierda WG, Castro JE, Aguillon R, et al. A phase I study of immune gene therapy for patients with CLL using a membrane-stable, humanized CD154. Leukemia 2010;24:1893–1900.
21. Melo-Cardenas J, Urquiza M, Kipps TJ, et al. Intratumoral delivery of CD154 homolog (Ad-ISF35) induces tumor regression: analysis of vector biodistribution, persistence and gene expression. Cancer Gene Ther 2012;19:336–344.
22. U.S. Department of Health and Human Services. *Guidance for Industry: Gene Therapy Clinical Trials—Observing Subjects for Delayed Adverse Events*. Food and Drug Administration, Center for Biologics Evaluation and Research, eds., 2006. www.fda.gov/downloads/BiologicsBloodVaccines/GuidanceComplianceRegulatoryInformation/Guidances/CellularandGeneTherapy/ucm078719.pdf
23. Applied Biosystems. *Creating Standard Curves with Genomic DNA or Plasmid DNA Templates for Use in Quantitative PCR* (Foster City, CA). 2003.
24. Rieger R, and Kipps TJ. CpG oligodeoxynucleotides enhance the capacity of adenovirus-mediated CD154 gene transfer to generate effective B-cell lymphoma vaccines. Cancer Res 2003;63:4128–4135.
25. Merrick AF, Shewring LD, Sawyer GJ, et al. Comparison of adenovirus gene transfer to vascular endothelial cells in cell culture, organ culture, and *in vivo*. Transplantation 1996;62:1085–1089.
26. Dirkx AE, Oude Egbrink MG, Wagstaff J, et al. Monocyte/macrophage infiltration in tumors: modulators of angiogenesis. J Leukoc Biol 2006;80:1183–1196.
27. Mantovani A, and Sica A. Macrophages, innate immunity and cancer: balance, tolerance, and diversity. Curr Opin Immunol 2010;22:231–237.
28. Thienel U, Loike J, and Yellin MJ. CD154 (CD40L) induces human endothelial cell chemokine production and migration of leukocyte subsets. Cell Immunol 1999;198:87–95.
29. Caux C, Massacrier C, Vanbervliet B, et al. Activation of human dendritic cells through CD40 cross-linking. J Exp Med 1994;180:1263–1272.
30. Caux C, Vanbervliet B, Massacrier C, et al. B70/B7-2 is identical to CD86 and is the major functional ligand for CD28 expressed on human dendritic cells. J Exp Med 1994;180:1841–1847.
31. Buhtoiarov IN, Lum H, Berke G, et al. CD40 ligation activates murine macrophages via an IFN-gamma-dependent mechanism resulting in tumor cell destruction *in vitro*. J Immunol 2005;174:6013–6022.
32. Rakhmilevich AL, Alderson KL, and Sondel PM. T-cell-independent antitumor effects of CD40 ligation. Int Rev Immunol 2012;31:267–278.
33. Henn V, Slupsky JR, Gräfe M, et al. CD40 ligand on activated platelets triggers an inflammatory reaction of endothelial cells. Nature 1998;391:591–594.
34. Chakrabarti S, Blair P, and Freedman JE. CD40-40L signaling in vascular inflammation. J Biol Chem 2007;282:18307–18317.
35. Zirlik A, Maier C, Gerdes N, et al. CD40 ligand mediates inflammation independently of CD40 by interaction with Mac-1. Circulation 2007;115:1571–1580.
36. Yang L, Debusk LM, Fukuda K, et al. Expansion of myeloid immune suppressor Gr+CD11b+ cells in tumor-bearing host directly promotes tumor angiogenesis. Cancer Cell 2004;6:409–421.
37. Pan PY, Ma G, Weber KJ, et al. Immune stimulatory receptor CD40 is required for T-cell suppression and T regulatory cell activation mediated by myeloid-derived suppressor cells in cancer. Cancer Res 2010;70:99–108.
38. Liljenfeldt L, Dieterich LC, Dimberg A, et al. CD40L gene therapy tilts the myeloid cell profile and promotes infiltration of activated T lymphocytes. Cancer Gene Ther 2014;21:95–102.

39. Grossmann ME, Brown MP, and Brenner MK. Antitumor responses induced by transgenic expression of CD40 ligand. Hum Gene Ther 1997;8:1935–1943.
40. Alderson MR, Armitage RJ, Tough TW, et al. CD40 expression by human monocytes: regulation by cytokines and activation of monocytes by the ligand for CD40. J Exp Med 1993;178:669–674.
41. MacGregor JN, Li Q, Chang AE, et al. *Ex vivo* culture with interleukin (IL)-12 improves CD8(+) T-cell adoptive immunotherapy for murine leukemia independent of IL-18 or IFN-gamma but requires perforin. Cancer Res 2006;66: 4913–4921.
42. Tomihara K, Kato K, Masuta Y, et al. Gene transfer of the CD40-ligand to human dendritic cells induces NK-mediated antitumor effects against human carcinoma cells. Int J Cancer 2007;120:1491–1498.
43. Woo EY, Chu CS, Goletz TJ, et al. Regulatory CD4(+) CD25(+) T cells in tumors from patients with early-stage non-small cell lung cancer and late-stage ovarian cancer. Cancer Res 2001;61:4766–4772.
44. Herndler-Brandstetter D, Schwaiger S, Veel E, et al. CD25-expressing CD8+ T cells are potent memory cells in old age. J Immunol 2005;175:1566–1574.

Address correspondence to:
Dr. Januario E. Castro
Moores Cancer Center
University of California–San Diego
3855 Health Sciences Drive # 0820
La Jolla, CA 92093-0820

E-mail: jecastro@ucsd.edu

Dr. Thomas J. Kipps
Moores Cancer Center
University of California–San Diego
3855 Health Sciences Drive # 0820
La Jolla, CA 92093-0820

E-mail: tkipps@ucsd.edu

Received for publication February 1, 2014;
accepted after revision October 21, 2014.

Published online: November 7, 2014.